Eur. Phys. J. B **16**, 647–651 (2000)

THE EUROPEAN PHYSICAL JOURNAL B

EDP Sciences

Er^{3+} spin relaxation and magnetic coupling in $ErNi_2B_2C$, $Er(Ni_{0.975}Co_{0.025})_2B_2C$ and $Er_{0.2}Y_{0.8}Ni_2B_2C$ from ^{166}Er Mössbauer measurements

J.A. Hodges[1,a], P. Bonville[1], H. Takeya[2], C. Godart[3], E. Alleno[3], G. Hilscher[4], H. Michor[4], M. El-Hagary[4], and A.M. Mulders[5]

[1] DRECAM-SPEC, Centre d'Études de Saclay, 91191 Gif-sur-Yvette, France
[2] National Institute for Metals, 1-2-1 Sengen, Tsukubara, Ibaraki, 305 Japan
[3] LCMTR-CNRS, Groupe des Laboratoires de Thiais, rue Henri-Dunant, 94320 Thiais, France
[4] Institut für Experimentalphysik, TU Wien, 1040 Wien, Austria
[5] IRI. T-U Delft, 2629 JB Delft, The Netherlands

Received 12 July 1999 and Received in final form 14 March 2000

Abstract. In a previous study of the Er^{3+} spin relaxation rate in $ErNi_2B_2C$ (Bonville *et al.*, Z. Phys. B **101**, 511 (1996)), we found that its thermal dependence showed an anomaly at the superconducting transition temperature ($T_c = 10.5$ K). This behaviour could be related either to a superconductivity-related change in the density of conduction band states to which the Er^{3+} spin is coupled or alternatively to the slowing down of the Er^{3+} spin fluctuations due to the development of short range magnetic order above the long range ordering temperature ($T_N \sim 6$ K). To identify the origin of the anomaly, we compared the results of a ^{166}Er Mössbauer study on $Er(Ni_{0.975}Co_{0.025})_2B_2C$ where T_c is depressed to 4 K and T_N remains near 6 K, and on $Er_{0.2}Y_{0.8}Ni_2B_2C$ where $T_c = 14.2$ K and there is no long range order. We conclude the relaxation anomaly is due to the onset of short range magnetic order. The normal state coupling of the $4f$-conduction electron exchange in the partially diluted sample is $|J_{kf}n(E_F)| = 0.015$. We also present ^{166}Er Mössbauer measurements of the hyperfine field in single crystal $ErNi_2B_2C$ which provide information concerning the direction of the magnetically ordered Er^{3+} moments in the superconducting phase.

PACS. 74.70.Dd Ternary, quaternary and multinary compounds (including Chevrel phases, borocarbides ets.) – 76.80.+y Mössbauer effect; other γ-ray spectroscopy

1 Introduction

Four of the rare earth borocarbides RNi_2B_2C (R = Tm, Er, Ho, Dy) show both superconductivity and rare earth sublattice magnetic order and all show some evidence of an interaction between the magnetically ordered rare earth sublattice and superconductivity [1–7]. The interplay between the two phenomena is most clearly evident for R = Ho where as the temperature is lowered, superconductivity appears, weakens and then strengthens again [1,8] and where the double re-entrance behaviour has been correlated with changes in the type of the Ho^{3+} sublattice magnetic order [2]. The exchange interactions between the different rare earth moments in the borocarbides are probably chiefly mediated by conduction electrons. Experimental measurements of the couplings of the rare earths with and through the conduction band in both the normal and superconducting phases are thus of interest.

We previously observed that the Er^{3+} spin fluctuation rate in $ErNi_2B_2C$ showed a linear temperature dependence above T_c (Korringa behaviour) and an anomalous drop as the temperature was lowered through T_c [9]. We suggested the anomaly could be linked to a superconductivity related reduction in the density of states which mediates the Er^{3+} spin fluctuations rate and we also mentioned the anomaly could be due to the onset of short range Er^{3+}-Er^{3+} magnetic correlations at a temperature fortuitously near T_c [9].

To better isolate the changes in the Er^{3+} spin fluctuation rates associated respectively with the superconducting transition and with short range magnetic order, we use cationic substitutions to independently modify T_c and T_N. We present the results of a ^{166}Er Mössbauer study of the thermal dependence of $1/T_1$ of Er^{3+} in $Er(Ni_{0.975}Co_{0.025})_2B_2C$ which has the same average T_N as $ErNi_2B_2C$ (~ 6 K) but with T_c reduced to 4 K and in $Er_{0.2}Y_{0.8}Ni_2B_2C$ where T_c is relatively high (14.2 K) and where there is no long range Er^{3+} magnetic order.

A further aspect of this study concerns the ^{166}Er Mössbauer measurement of the directions of the Er^{3+} moments in single crystal $ErNi_2B_2C$ at 1.4 K. Neutron diffraction

[a] e-mail: hodges@spec.saclay.cea.fr

measurements on polycrystalline $ErNi_2B_2C$ have shown the Er^{3+} moments are colinear and lie in the basal plane [10–12] and magnetisation measurements on single crystal $ErNi_2B_2C$ have shown that below 2.2 K, the Er^{3+} are weakly non colinear [16].

2 Experimental details

The polycrystalline $ErNi_2B_2C$ and $Er(Ni_{0.975}Co_{0.025})_2B_2C$ samples were prepared by melting the constituent elements (Er(purity 99.9%)), Ni(99.9%), Co(99.9%), B(99.7%), C(99.997%) in a two step procedure described previously [17]. The samples were annealed in an evacuated quartz tube at 800 °C ($ErNi_2B_2C$) or 900 °C ($Er(Ni_{0.975}Co_{0.025})_2B_2C$) for 14 days. The X-ray diffraction analyses gave the following results: $ErNi_2B_2C$; $a = 3.502$, $c = 10.563$ Å (no detectable impurities), $Er(Ni_{0.975}Co_{0.025})_2B_2C$; $a = 3.501$, $c = 10.555$ Å (impurities $Er_2Ni_3B_6$(4%), ErB_2C_2(3%), unidentified(4%)). The $Er_{0.2}Y_{0.8}Ni_2B_2C$ sample was synthesized using erbium enriched in the Mössbauer isotope ^{166}Er by high frequency induction melting in an argon atmosphere. The melting was repeated 12 times to ensure optimum homogeneity. The sample was then annealed at 1020 °C for one week. The X-ray analysis provided the lattice parameters, $a = 3.5229$, $c = 10.5473$ Å, and showed there were no detectable impurities.

Single crystal $ErNi_2B_2C$ was grown by the floating zone method previously used to provide single crystals of YNi_2B_2C and of $HoNi_2B_2C$ [13,14]. The growth speed was near 1.0 mm/h in flowing argon and the final boule was 80 mm long and 6 mm diameter. X-ray measurements on the crushed powder sample showed there were no detectable impurity phases.

Mössbauer measurements were made on ^{166}Er ($I_g = 0$, $I_{ex} = 2$, $E_\gamma = 80.6$ keV, 1 mm/s = 65 MHz) using a source of neutron irradiated $^{166}Ho^*_{0.4}Y_{0.6}$ H_2 (half-life 27 h) and a triangular velocity sweep.

3 Magnetic moment direction in $ErNi_2B_2C$

The transition probabilities of the different Mössbauer transitions ($\Delta m_I = \pm 2, \pm 1, 0$ for ^{166}Er) of a hyperfine field spectrum depend on the angle between the γ-ray propagation direction and the direction of the local quantisation axis which is defined by the direction of the hyperfine field [18]. The direction of this field corresponds to the direction of the Er^{3+} magnetic moment. When the angle between the γ-ray propagation direction and the crystal c-axis is known, the measurement of the relative intensities of the different transitions provides the direction of the moments relative to this axis.

Figure 1 shows the Mössbauer absorption pattern obtained at 1.4 K for a single crystal sample of $ErNi_2B_2C$ with the γ-rays propagating along the crystal c-axis. For comparison, the figure also recalls the data for the polycrystalline sample [9]. With respect to the directional properties of the hyperfine field, the two main features

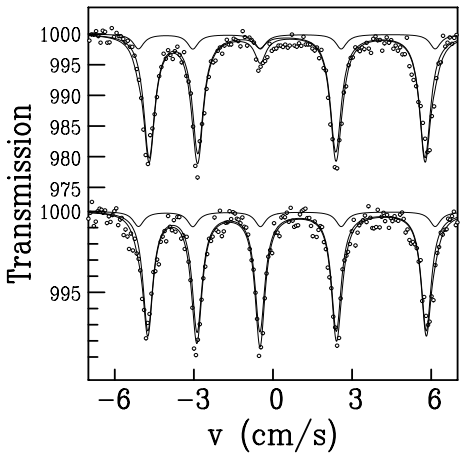

Fig. 1. ^{166}Er Mössbauer absorption in $ErNi_2B_2C$ at 1.4 K. Top: single crystal sample with the γ-rays along the crystal c-axis. Bottom: polycrystalline sample [9]. In both cases the weak subspectrum is related to the Er^{3+} at sites with modified crystal field properties.

of the lineshape for the single crystal sample are the very much reduced intensity of the central line and the essentially equivalent intensities of the four outer components. These features show the Er^{3+} moments are close to perpendicular to the the γ-ray propagation direction, that is they are perpendicular to the crystal c-axis. We note however, that the central component is not absent as it would be if the moments were exactly perpendicular to the γ-ray direction. It is probable that part of the intensity of this central component is associated with the central component of the well split five line subspectrum which continues to exist above the magnetic ordering temperature and which has an intensity about 15% of that of the main spectrum. (A similar subspectrum which we called the "secondary component" is also present in our polycrystalline $ErNi_2B_2C$ sample and indeed, it is also present in all the different Er borocarbides we have examined [9,19]. It is not due to Er^{3+} in any impurity phases and it may be due to Er^{3+} at sites with modified crystal field properties.) Taking this secondary component into account, and allowing for the various experimental uncertainties linked with sample and γ-ray alignment, we find the Er^{3+} moments are essentially perpendicular to the crystal c-axis with an uncertainty of 6°. This result is compatible with the ordered direction found by neutron diffraction (moments perpendicular to the c-axis) [10–12] but the uncertainties are too high to be able to confirm or disprove the canting of about 3° suggested by the magnetisation measurements [16].

4 Spin relaxation rates in $Er(Ni_{0.975}Co_{0.025})_2B_2C$

The presence of 2.5% Co reduces T_c to 4 K [19] so confirming the strong dependence of T_c on Co substitution level seen in other borocarbides [8,20]. $^{166}Er^{3+}$ Mössbauer absorption measurements were made over the range 1.4

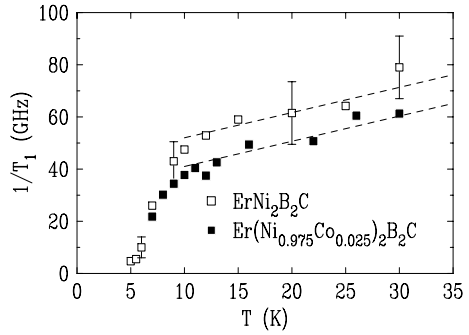

Fig. 2. From ^{166}Er Mösbauer measurements: thermal dependence of the Er^{3+} spin relaxation rates in $ErNi_2B_2C$ (T_c = 10.5 K) [9] and $Er(Ni_{0.975}Co_{0.025})_2B_2C$ ($T_c = 4$ K). Each fitted dashed straight line represents the sum of a constant spin-spin term, a linear Korringa law and a Hirst-Orbach law (see text).

to 30 K. The saturated hyperfine field of 720(20) T is directed essentially perpendicular to the principal axis of the electric field gradient, T_N has an average value of ~ 6 K and there is a distribution in the local values over the range 4 to 7 K. All these characteristics are the same as for $ErNi_2B_2C$ [9]. In the range 7 to 20 K, the lineshapes were fitted with the longitudinal fluctuation model used previously [9] and the obtained spin relaxation rates are shown in Figure 2. For comparison, this figure also recalls the equivalent rates for $ErNi_2B_2C$ [9]. For both compounds, we observe a pronounced anomaly near 10 K and a quasi-linear thermal dependence above. The anomaly thus remains at the same temperature for the two samples with their quite different values of T_c (10 and 4 K). The relaxation rate anomaly is thus not coupled with T_c and so must be attributed to the the slowing down of the spin fluctuations associated with the onset of Er^{3+} short range magnetic correlations.

Although the major part of the anomaly at 10 K is due to short range order, a small anomaly, due to a change in coupling with the conduction band states, could possibly still exist at T_c. To investigate this, it is necessary to improve the experimental sensitivity to small changes in the rate by reducing the "background" relaxation rate coming from the Er^{3+} spin-spin coupling. To this end, we carried out measurements on a superconducting sample with a reduced Er^{3+} concentration level.

5 Spin relaxation rates in $Er_{0.2}Y_{0.8}Ni_2B_2C$

The T_c value of 14.2 K is intermediate between that for YNi_2B_2C (15.5 K) and $ErNi_2B_2C$ (10.5 K) and it scales almost linearly with the Y/Er composition ratio. Our use of the reduced Er^{3+} concentration level reduces the "background" spin-spin rate to about 5% of that in $ErNi_2B_2C$ (see below). It would be possible to reduce this contribution further by using even lower concentration levels, but then it would be difficult to carry out a Mössbauer study because of the decreased signal to noise ratio.

The Mössbauer spectra, obtained in a range (1.5 to 20 K) englobeing T_c, are given in Figure 3 which shows

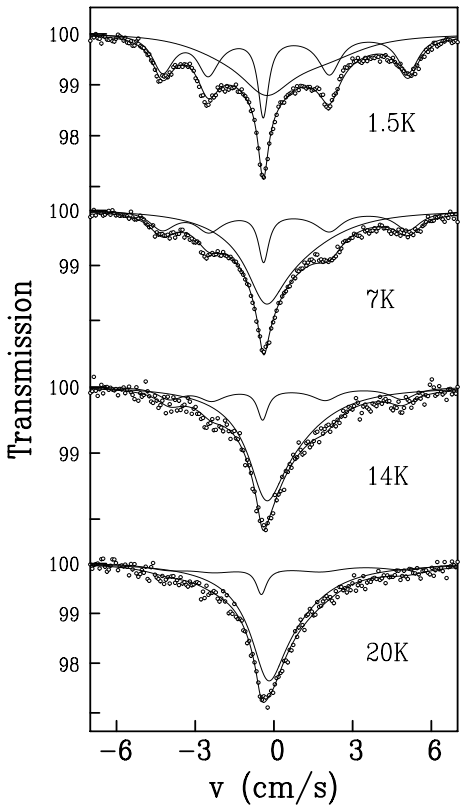

Fig. 3. ^{166}Er Mössbauer absorption in $Er_{0.2}Y_{0.8}Ni_2B_2C$ fitted in terms of two subspectra as described in the text.

that the well defined structure visible at 1.5 K progressively disappears as the temperature is increased. At all temperature in the examined range, we find it is not possible to fit the data in terms of a single set of hyperfine parameters showing that different local properties coexist. We find the assumption of just two subspectra is enough to obtain good quality data fits at all temperatures. This assumption thus mimics quite well the range of local properties that is really present and which arises due to the inherent statistical variation in the local Er^{3+} concentration level. As shown in Figure 3, one subspectra has five more or less resolved lines and the other takes the form of a single broad line. We attribute the two subspectra respectively to regions where the local density of the Er^{3+} is "concentrated" or "dilute". The five line subspectrum was fitted assuming the Er^{3+} behave as in $ErNi_2B_2C$ in its magnetically ordered state whereas the single line subspectrum was fitted assuming the Er^{3+} behave as in $ErNi_2B_2C$ above its magnetic ordering temperature [9]. In the region near T_c, this latter subspectrum strongly dominates and it amounts to 75-80% of the total spectral weight. (At T_c, the major part of the remaining spectral weight is probably associated with the Er^{3+} having locally modified crystal field parameters (the "secondary component").) The thermal dependence of the spin relaxation rate for the two subspectra are given in Figure 4. Neither the dominant subspectrum ("dilute regions") nor the minor subspectrum ("concentrated regions") show any evidence of an anomaly

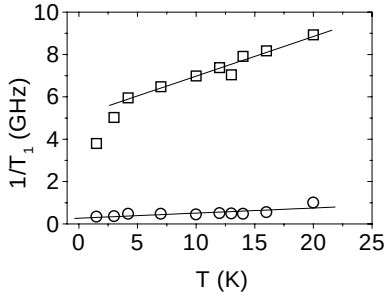

Fig. 4. From ^{166}Er Mösbauer measurements: thermal dependence of the Er^{3+} spin relaxation rates in $Er_{0.2}Y_{0.8}Ni_2B_2C$ ($T_c = 14.5$ K) where two subspectra are visible. The dominant subspectrum provides the values shown by the open squares and the associated fitted straight line represents the sum of a constant spin-spin term, a linear Korringa law and a Hirst-Orbach law. The minority subspectrum (see text) provides the values shown by the open circles.

in the spin relaxation rate at T_c. There is thus no evidence of any coupling of the Er^{3+} spins to electronic states whose properties change at the superconducting transition.

Despite minor incoherences in this two subspectrum treatment (the relative weights of the two subspectra depend slightly on the temperature, the 5 line subspectrum continues to exist to temperatures above the known T_N for the concentrated Er^{3+} compounds so that it cannot be entirely due to the continued presence of magnetic interactions), the analysis clearly shows there is no evidence of a relaxation rate anomaly at T_c. In fact, whatever the precise method followed for any quantitative analysis, no anomaly will appear in the values the spin relaxation rates. Also, the fact that there is no visible anomaly in the evolution of the bare Mössbauer absorption lineshapes already evidences against any anomaly. This contrasts with the behaviour in $ErNi_2B_2C$ where the anomaly seen in the fitted relaxation rates is also apparent as a clear anomaly in the evolution of the bare Mössbauer absorption lineshapes.

To obtain a numerical value for the $4f$-conduction electron exchange, we consider the behaviour of the dominant single line subspectrum and following the same procedure adopted for $ErNi_2B_2C$ [9], we fit the relaxation rate in the linear region above 4 K to the expression

$$\frac{1}{T_1} = \left(\frac{1}{T_1}\right)_0 + C_K T + \left(\frac{1}{T_1}\right)_{HO}$$

where $(1/T_1)_0$ can be interpreted as the average exchange spin-spin relaxation rate and $C_K T$ is the average Korringa relaxation rate due to the exchange between the localised $4f$ electrons and the conduction band, $(1/T_1)_{HO}$ is a Hirst-Orbach contribution involving the ground and first excited CEF levels. We obtain a value of $(1/T_1)_0 = 2.2$ GHz which is 5% of that in $ErNi_2B_2C$. This reduction in the spin-spin relaxation rate is directly due to the lowered Er^{3+} concentration. We find $|J_{kf} n(E_F)| = 0.015$, which falls in the range previously observed for Er^{3+} substituted into simple metals [22] and it is about 50% of our initial value for $ErNi_2B_2C$ [9]. This reduction is probably too important to be attributed to changes in J_{kf} or in $n(E_F)$ caused by partially substituting Y^{3+} for Er^{3+}. We suggest that it mainly arises because our value for $|J_{kf} n(E_F)|$ in $ErNi_2B_2C$ was overestimated. In our previous analysis, we assumed the spin-spin interaction was independent of temperature but because there are a number of relatively low lying crystal field levels [15,21], it will rather increase with increasing temperature as the excited crystalline field levels become thermally populated. In other words, the increase in the relaxation rates in $ErNi_2B_2C$ with increasing temperature (recalled in Fig. 2) is due to a thermally dependent spin-spin interaction as well as to the Korringa and Hirst-Orbach mechanisms. The present results show that a more reliable value for $|J_{kf} n(E_F)|$ may be obtained from measurements on the sample with low Er^{3+} concentration levels where the spin-spin interaction is reduced.

6 Conclusions

By comparing ^{166}Er Mössbauer measurements in $ErNi_2B_2C$, $Er(Ni_{0.975}Co_{0.025})_2B_2C$ and $Er_{0.2}Y_{0.8}Ni_2B_2C$, we find there is no anomaly in the Er^{3+} spin fluctuation rate at T_c attributable to an anomaly in the coupling between the Er^{3+} spin and a conduction band. A clear anomaly in the coupling is however evidenced by the NMR ^{11}B spin lattice relaxation rate in, for example, YNi_2B_2C. [23]. We also observe that substituting Co into $ErNi_2B_2C$ to obtain $Er(Ni_{0.975}Co_{0.025})_2B_2C$ has no discernable influence on the thermal dependence of the Er^{3+} spin fluctuation rate above T_c, even though the presence of Co is known to reduce the overall density of states at the Fermi level [20]. Both these results suggest that despite the known interplay between superconductivity and Er^{3+} sublattice magnetic order in the borocarbides, the coupling to the electronic states within the Er^{3+} sublattice and the coupling to electronic states within the Ni-B layer remain relatively independent.

References

1. H. Eisaki, H. Takagi, R.J. Cava, B. Batlogg, J.J. Krajewski, W.F. Peck Jr., K. Mizuhashi, J.O. Lee, S. Uchida, Phys. Rev. B **50**, 647 (1994).
2. T.E. Grigereit, J.W. Lynn, Q. Huang, A. Santoro, R.J. Cava, J.J. Krajewski, W.F. Peck Jr, Phys. Rev. Lett. **73**, 2756 (1994).
3. B. K. Cho, P.C. Canfield, D.C. Johnston, Phys. Rev. B **52**, R3844 (1995).
4. Z.Q. Peng, K. Krug, K. Winzer, Phys. Rev. B **57**, R8123 (1998).
5. B.K. Cho, M. Xu, P.C. Canfield, L.L Miller, D.C. Johnston, Phys. Rev. B **52**, 3676 (1995).
6. L.J. Chang, C.V. Tomy, D. McK. Paul, C. Ritter, Phys. Rev. B **54**, 9031 (1996).
7. B.K. Cho, P.C. Canfield, L.L. Miller, D.C. Johnston, W.P. Beyermann, A. Yatskar, Phys. Rev. B **52**, 3684 (1995).
8. E. Tominez, E. Alleno, C. Godart, P. Bonville, J.A. Hodges, J. Alloys Compounds **262-263**, 462 (1997).

9. P. Bonville, J.A. Hodges, C. Vaast, E. Alleno, C. Godart, L.C. Gupta, Z. Hossain, R. Nagarajan, Z. Phys. B **101**, 511 (1996).
10. J. Zaretsky, C. Stassis, A.I. Goldman, P.C. Canfield, P. Dervengas, B.K. Cho, D.C. Johnston, Phys. Rev. B **51**, 678 (1995).
11. S.K. Sinha, J.W. Lynn, T.E. Grigereit, Z. Hossain, L.C. Gupta, R. Nagarajan, C. Godart, Phys. Rev. B **51**, 681 (1995).
12. J.W. Lynn, S. Skanthakumar, Q. Huang, S.K. Sinha, Z. Hossain, L.C. Gupta, R. Nagarajan, C. Godart, Phys. Rev. B **55**, 6584 (1997).
13. H. Taketa, T. Hirano, K. Kadowaki, Physica C **256**, 220 (1996).
14. H. Taketa, K. Kadowaki, K.Hirata, T. Hirano, J. Alloys Compounds **245**, 94 (1996).
15. U. Gasser, P. Allenspach, F. Fauth, W. Henggeler, J. Mesot, A. Furrer, S. Rosenkranz, P. Vorderwisch, M. Buchgeister, Z. Phys. B **101**, 345 (1996).
16. P.C. Canfield, S.L. Bud'ho, B.K. Cho, Physica C **262**, 248 (1996).
17. E. Alleno, Z. Hossain, C. Godart, R. Nagarajan, L.C. Gupta, Phys. Rev. B **52**, 7428 (1995).
18. J.W. Robinson, *Handbook of Spectroscopy* (CRC Press, 1981), Vol. III, p. 451.
19. P. Bonville, J.A. Hodges, C. Vaast, E. Alleno, C. Godart, L.C. Gupta, R. Nagarajan, Physica B **223-224**, 72 (1996).
20. H. Schmidt, H.F. Braun, Phys. Rev. B **55**, 8497 (1997).
21. S. Süllow, B. Ludoph, C.E. Snel, F.E. Kayzel, E. Brück, G.J. Nieuwenhuys, A.A. Menovsky, J.A. Mydosh, Z. Phys. B **98**, 17 (1995).
22. D. Davidov, R. Orbach, C. Rettori, D. Shaltiel, L.J. Tao, B. Ricks, Phys. Lett. A **35**, 339 (1971).
23. F. Borsa, Q. Hu, K.H. Kim, D.R. Torgenson, P. Canfield, M. Xu, B. Zhong, Physica C **235-240**, 1547 (1994).